JOURNAL OF GEOPHYSICAL RESEARCH, VOL. 105, NO. D16, PAGES 20,773–20,790, AUGUST 27, 2000

Radiative forcings and global warming potentials of 39 greenhouse gases

Atul K. Jain,[1] Bruce P. Briegleb,[2] K. Minschwaner,[3] and Donald J. Wuebbles[1]

Abstract. The radiative forcings and global warming potentials for 39 greenhouse gases are evaluated using narrowband and broadband radiative transfer models. Unlike many previous studies, latitudinal and seasonal variations are considered explicitly, using distributions of major greenhouse gases from a combination of chemical-transport model results and Upper Atmosphere Research Satellite (UARS) measurements and cloud statistics from the International Satellite Cloud Climatology Project. The gases examined include CO_2, CH_4, N_2O, plus a number of chlorofluorocarbons, hydrochlorofluorocarbons, hydrofluorocarbons, hydrochlorocarbons, bromocarbons, iodocarbons, and perfluorocarbons (PFCs). The model calculations are performed on a 5° latitude grid from 82.5°S to 82.5°N. The radiative forcings determined by the model are then used to derive global warming potential for each of the compounds, which are compared with prior analyses. In addition, the latitudinal and seasonal dependence of radiative forcing since preindustrial time is calculated. The vertical profiles of the gases are found to be important in determining the radiative forcings; the use of height-independent vertical distributions of greenhouse gases, as used in many previous studies, produce errors of several percent in estimated radiative forcings for gases studied here; the errors for the short-lived compounds are relatively higher. Errors in evaluated radiative forcings caused by neglecting both the seasonal and the latitudinal distributions of greenhouse gases and atmospheres are generally smaller than those due to height-independent vertical distributions. Our total radiative forcing due to increase in major greenhouse gas concentrations for the period 1765-1992 is 2.32 Wm^{-2}, only 2% higher than other recent estimates; however, the differences for individual gases are as large as 23%.

1. Introduction

Radiative forcing, expressed as the change in radiative energy flux in units of Wm^{-2}, is a useful measure of the climate change impact expected from changing concentrations of greenhouse gases (CO_2, CH_4, N_2O, H_2O, O_3, and halocarbons) and aerosols. While radiative forcing can be calculated with more confidence than the response of climate in terms of global and regional temperature change, care must be taken where large seasonal and/or regional variations exist in the anthropogenic and natural factors affecting the radiative forcing. Previous estimates of the radiative forcings for several greenhouse gases have been published, with relatively large differences in the results [*Hansen et al.*, 1997; *Minschwaner et al.*, 1998; *Good et al.*, 1998; *Myhre and Stordal*, 1997; *Myhre et al.*, 1998; *Naik et. al.*, 2000; *Pinnock et al.*, 1995; *Freckleton et al.*, 1998, and references therein]. This may be due to the fact that the estimates had been carried out using a range of different types of radiative transfer models and a diverse set of data sources. In the absence of a coherent set of radiative forcing estimates, even the international assessments, such as the Intergovernmental Panel on Climate Change [*Schimel et al.*, 1996] and World Meteorological Organization [*Granier et al.*, 1999], used these diverse results for their assessment of greenhouse warming impact.

The purpose of this paper is to examine the radiative forcings and the global warming potentials (GWPs) of a wide range of greenhouse gases using a consistent set of radiative transfer models, in addition to spectroscopic and climate data sets. The gases examined here include the most common greenhouse gases (CO_2, CH_4, and N_2O) as well as a number of halocarbons and perfluorocarbons (SF_6, CF_4). First, we evaluate the radiative forcings due to a single global and annual mean (GAM) profile of temperature, water vapor (H_2O), ozone (O_3), cloudiness, and greenhouse gas concentrations using broadband (BBM) and narrowband (NBM) radiative transfer models. Our motivation here is to examine the sensitivity of greenhouse gas radiative forcings to a number of simplified assumptions widely used in past calculations. Since there are large spatial and temporal variations in climate data, we next calculate the radiative forcings of the greenhouse gases considered in this study as a function of latitude and season using the NBM. Third, we examine the radiative forcings of a number of greenhouse gases since preindustrial times as a function of latitude and season. In the past, simplified expressions relating the radiative forcings to the changes in the greenhouse gas concentrations were used for this type of evaluation [*Shine et al.*, 1990; *Schimel et al.*, 1996]. In contrast, we have estimated the radiative forcing using the NBM as well as using the distributions of major greenhouse gases based on a combination of atmospheric model calculations and UARS measurements. Finally, we evaluate the GWPs for the 39 gases considered here on the basis of our "best estimate" values of radiative forcings.

[1] Department of Atmospheric Sciences, University of Illinois at Urbana-Champaign.
[2] National Center for Atmospheric Research, Boulder, Colorado.
[3] Department of Physics, New Mexico Institute of Mining and Technology, Socorro.

Paper number 2000JD900241.
0148-0227/00/2000JD900241$09.00

Section 2 provides a brief description of the method used to calculate radiative forcings using radiative transfer models, along with a discussion of the climate and the spectroscopic data sets used in this study. In section 3 we report the global mean radiative forcing results for various sensitivity tests based on a single GAM atmosphere. Section 4 discusses the radiative forcing results for major greenhouse gases based on latitudinal and seasonal atmospheres since preindustrial times. In section 5 we compare the observation-based and CTM-based (chemical-transport model) radiative forcings. Section 6 compares the NBM-calculated radiative forcings for various greenhouse gases with other recent research studies. The estimated GWPs based on our "best estimates" of radiative forcings are discussed in section 7. Finally, the major findings of this study are summarized in section 8.

2. Method, Models, and Input Data

2.1. Method

The purpose of this paper is to calculate the radiative forcing of a number of greenhouse gases using a consistent set of radiative transfer models and data sets, which are discussed in detail in following sections. Radiative forcing is calculated as the change in net irradiance due to a change in greenhouse gas concentrations at the tropopause after allowing for the adjustment of stratospheric temperatures to radiative equilibrium [*Schimel et al.*, 1996; *Granier et al.*, 1999]. The adjustment of the stratosphere is included because the stratosphere responds in a few months, whereas the surface-troposphere system responds in decades due to the large thermal inertia of the ocean. The radiative forcing that we have calculated here, taking this adjustment into account, is called the adjusted radiative forcing. If the stratospheric adjustment is not accounted for, the derived radiative forcing is called the instantaneous radiative forcing. We explicitly consider the latitudinal and seasonal variations using zonally and seasonally averaged distributions of temperature, H_2O, O_3, trace gases, and clouds.

As discussed by *Myhre and Stordal* [1997] and *Freckleton et al.* [1998], the tropopause height and definition (i.e., lapse rate criteria, temperature minimum, and top of convective layer) are crucial in determining the magnitude of radiative forcing. *Myhre and Stordal* [1997] show that assuming a fixed global-mean tropopause height for each latitude belt can produce errors of up to 10% in the instantaneous global-mean forcing. Moreover, *Freckleton et al.* [1998] have shown that the choice of tropopause definition can influence the radiative forcing results by up to 9%. In this study we define the tropopause at each latitude as a level where the minima in temperature occurs.

2.2. Distributions of H_2O, O_3, Temperature, and Clouds

The vertical profiles of temperature, H_2O, and O_3 are important parameters in the calculations of radiative forcing. In this study, latitudinal and seasonal variations of temperature, H_2O, O_3, and clouds are based on in situ and satellite data. Here we provide only the brief description of the data used. A detailed description of the data used in this study can be found in the work of *Minschwaner et al.* [1998].

Distributions of H_2O, O_3, and temperature, along with the cloud fraction and heights assumed in the calculations for the September-October time period, are shown in Plate 1. Zonally averaged distributions of temperature, H_2O, and O_3 in the stratosphere were compiled on the basis of UARS Microwave Limb Sounder measurements [*Waters et al.*, 1993] over 2 month periods covering the equinoxes and solstices. The total time interval extends from March 1992 to January 1993. Temperature profiles in the troposphere were adopted from the National Meteorological Center analysis [*McPherson et al.*, 1979]. O_3 in the troposphere was based on the climatological values from *Oltmans* [1981] and *Levy et al.* [1985], while tropospheric H_2O was specified on the basis of standard Air Force Geophysics Laboratory (AFGL) models [*Anderson et al.*, 1986]. We adopted the values for the cloud fractions for low, middle, and high clouds from the International Satellite Cloud Climatology Project (ISCCP) [*Rossow and Schiffer*, 1991]. Low clouds are assumed to be located between 850 and 750 mbar, middle-level clouds are placed in a 100-mbar-thick layer centered near 500 mbar at middle and high latitudes, and near 550 mbar in tropics. High clouds are located in a 20-mbar-thick layer located just below the tropopause. The values for cloud liquid water paths and effective drop radii for the three cloud types assumed in this study were taken from *Stephens and Platt* [1987], consistent with the values used by *Dessler et al.* [1996]. Surface emissivity was assumed to be fixed at 0.92, independent of latitude and season. This value represents an estimate of the weighted mean of sea surface, sand, and snow. Calculated forcings were found to be relatively insensitive to the precise choice of surface longwave emissivity.

2.3. Model-Estimated and Observed Concentrations for Trace Gases

To examine the sensitivity of the radiative forcing to vertical, latitudinal, and seasonal greenhouse gas distribution, two changes were considered: (1) uniform changes throughout the atmosphere for all seasons (UCA), and (2) height-dependent changes in the vertical profile as well as latitudinal and seasonal changes in vertical profiles (NUCA). The radiative forcings for UCA were estimated for a uniform increase of 5 ppmv for CO_2 (350 to 355 ppmv), 10 ppbv for CH_4 (1714 to 1724 ppbv), and N_2O (311 to 321 ppbv). In order to reduce the error due to nonlinear absorption caused by a weak line limit for halocarbons and perfluorocarbons, the forcings were calculated for a 0.1 ppbv (zero to 0.1 ppbv) change. For the NUCA case the radiative forcings were calculated for an increase in greenhouse gas concentrations from preindustrial times to the present-day time period (1992). The latitudinal, seasonal, and vertical distributions of all greenhouse gases, with the exception of CO_2, CFC-13, perfluorocarbons (PFCs), iodocarbons (ICs) and three bromocarbons (CH_3Br, CH_2Br_2, and CHF_2Br), were calculated using a two-dimensional (latitude and altitude) chemical-transport model (CTM) of the global atmosphere [*Naik et al.*, 2000; *Wuebbles et al.*, 2000; *Kotamarthi et al.*, 1999]. This model has been used extensively in past international ozone assessments to determine lifetimes of halocarbons and other greenhouse gases and their effects on ozone [*WMO*, 1992, 1995]. The model grid is 5° in latitude from pole to pole and about 1.5 km in altitude from the surface to 85 km. The preindustrial and present-day concentrations were calculated for fixed surface concentration boundary conditions, which were taken from *Schimel et al.* [1996]. The preindustrial surface concentrations for all halocarbons were assumed to be zero. The current concentrations for all of the HCFCs (except for HCFC-22) and HFCs are also zero. However, to evaluate the sensitivity of radiative forcing to the variation in vertical profile, the 1992 concentrations for these compounds were calculated by assuming the surface concentration of 5 pptv. Generally, the radiative forcings for halocarbons are reported for a 1 ppbv increase; hence our results for the UCA and NUCA cases were rescaled to reflect the impact of a 1 ppbv change in halocarbon concentrations.

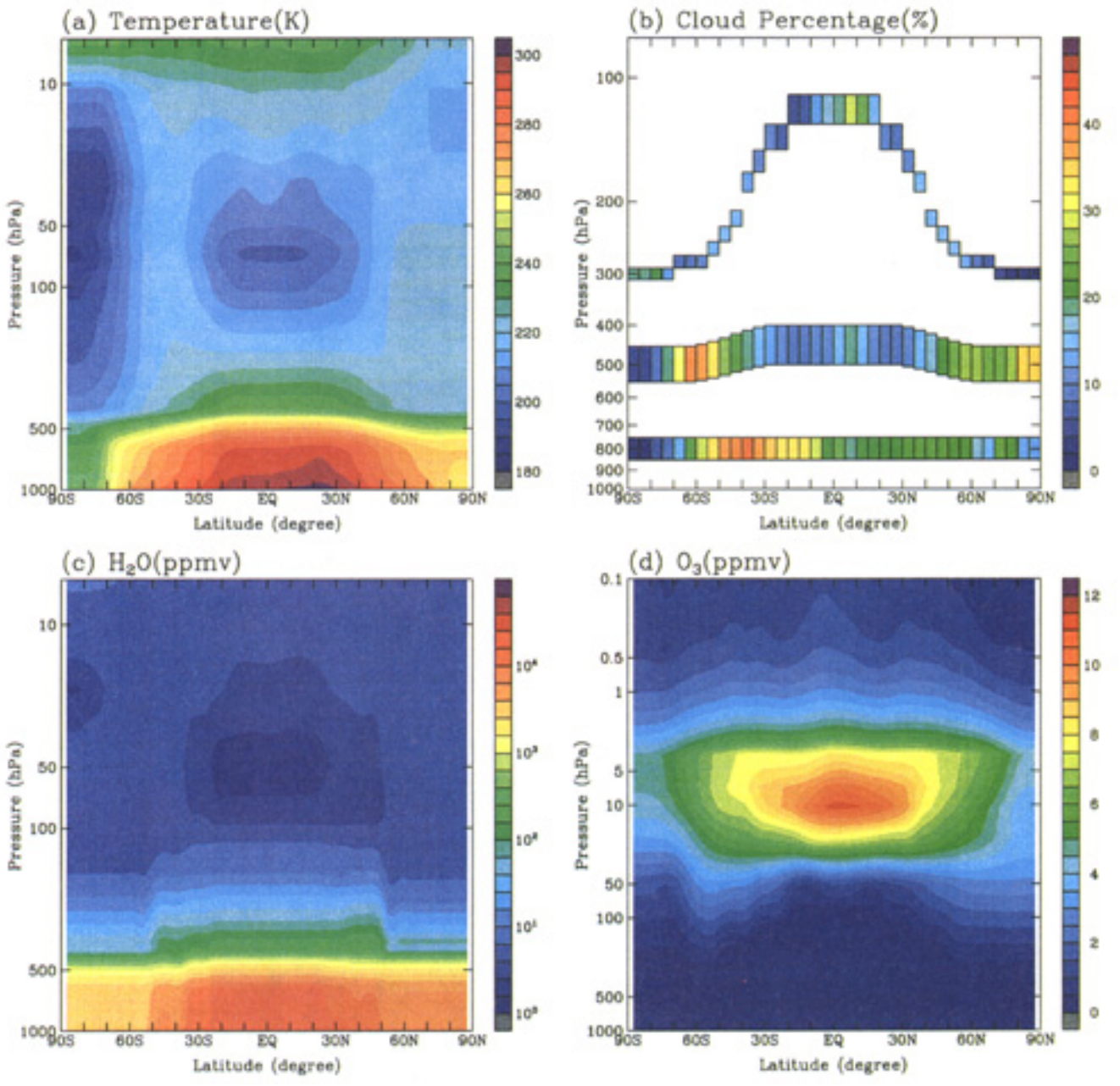

Plate 1. Distributions of (a) temperature (K), (b) cloud fractions (percent), (c) H_2O (ppmv), and (d) O_3 (ppmv) used in the radiative calculations for the September-October preindustrial and contemporary time periods.

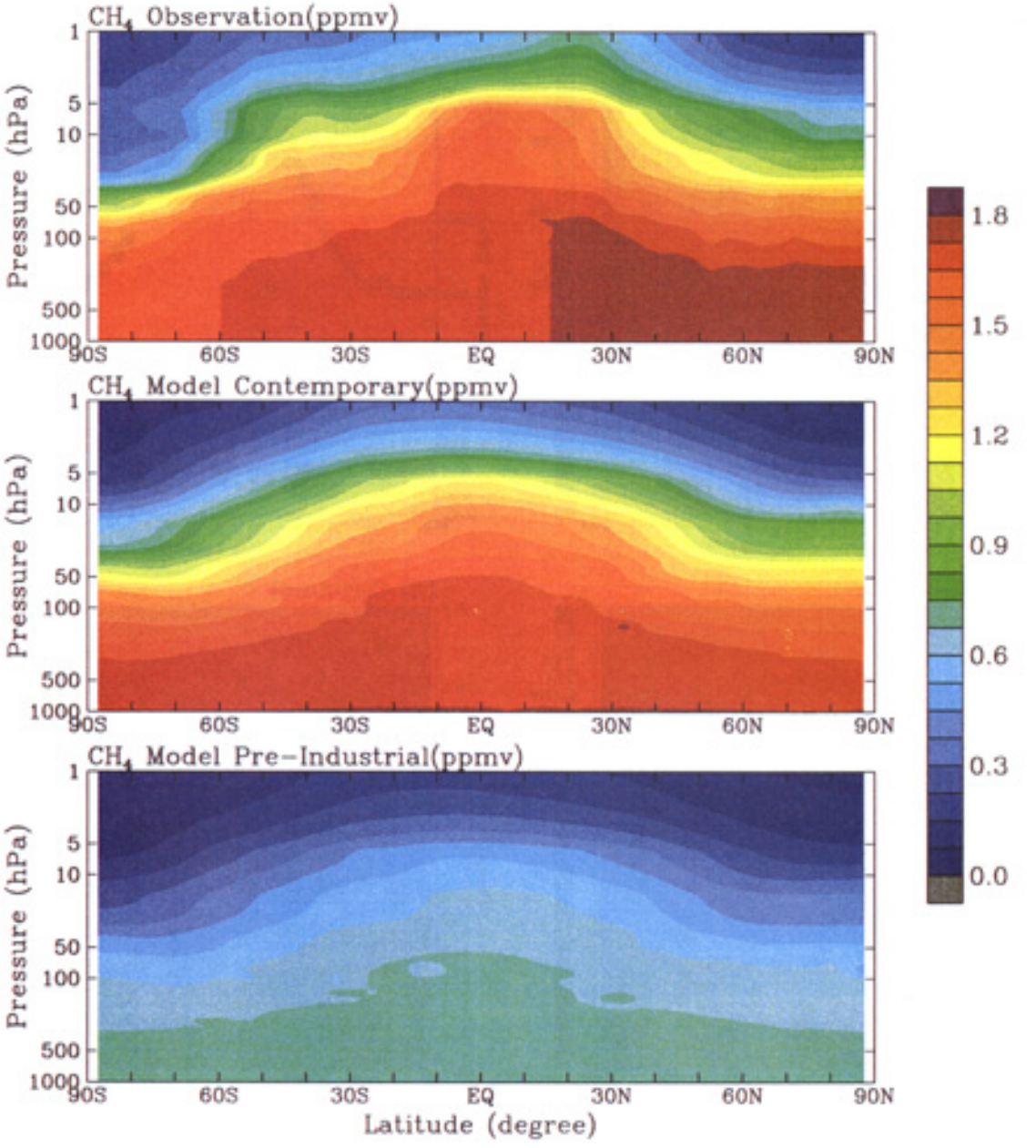

Plate 2. Chemical transport model- (CTM) estimated and observed distribution of CH_4 (ppmv) used in the radiative calculations for the September-October contemporary period. Plate also shows the CTM-estimated CH_4 distributions that were used for the September-October preindustrial time period.

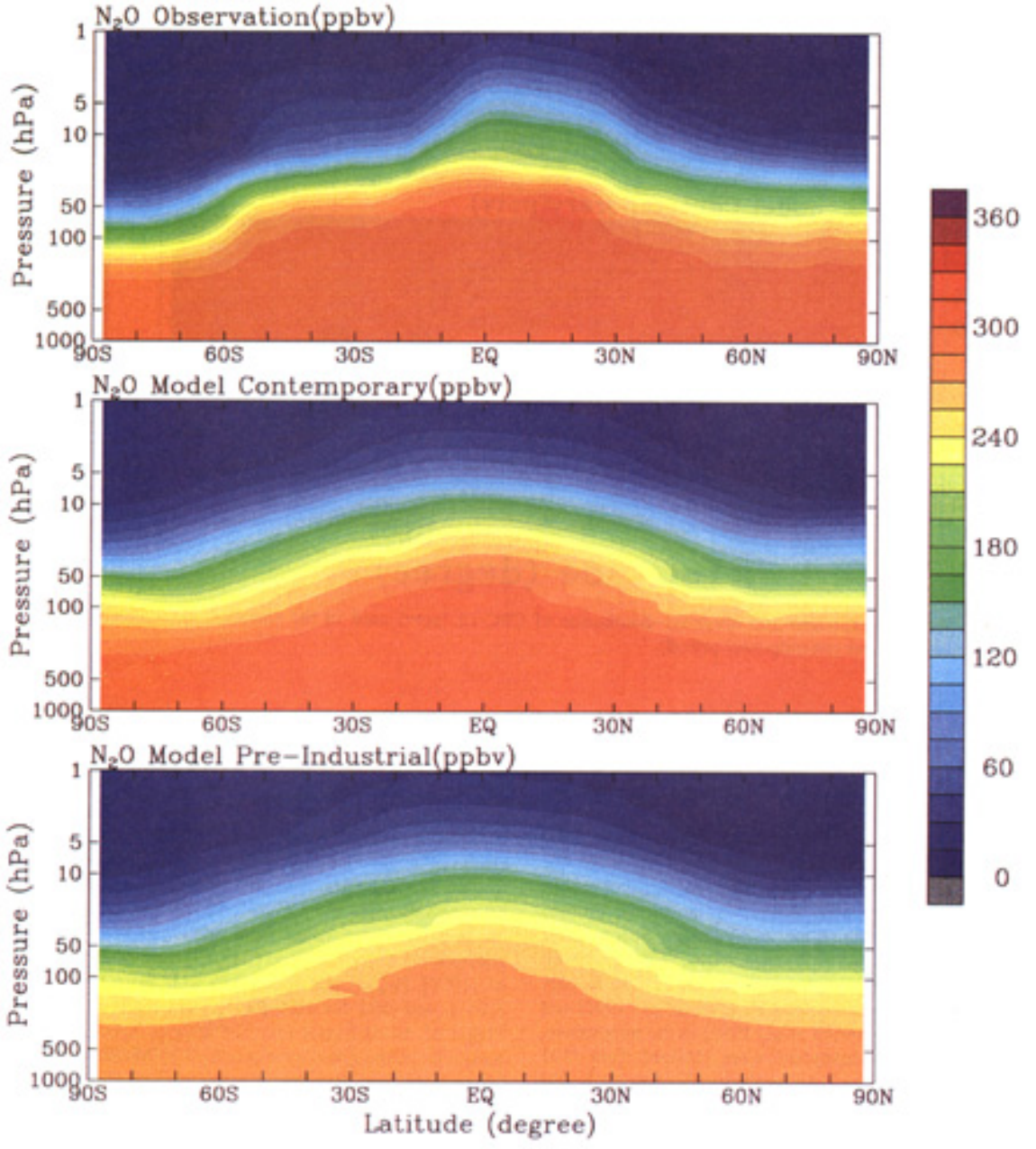

Plate 3. CTM-estimated and observed distribution of N_2O (ppbv) used in the radiative calculations for the September-October contemporary period. Plate also shows the CTM-estimated N_2O distributions used for the September-October preindustrial time period.

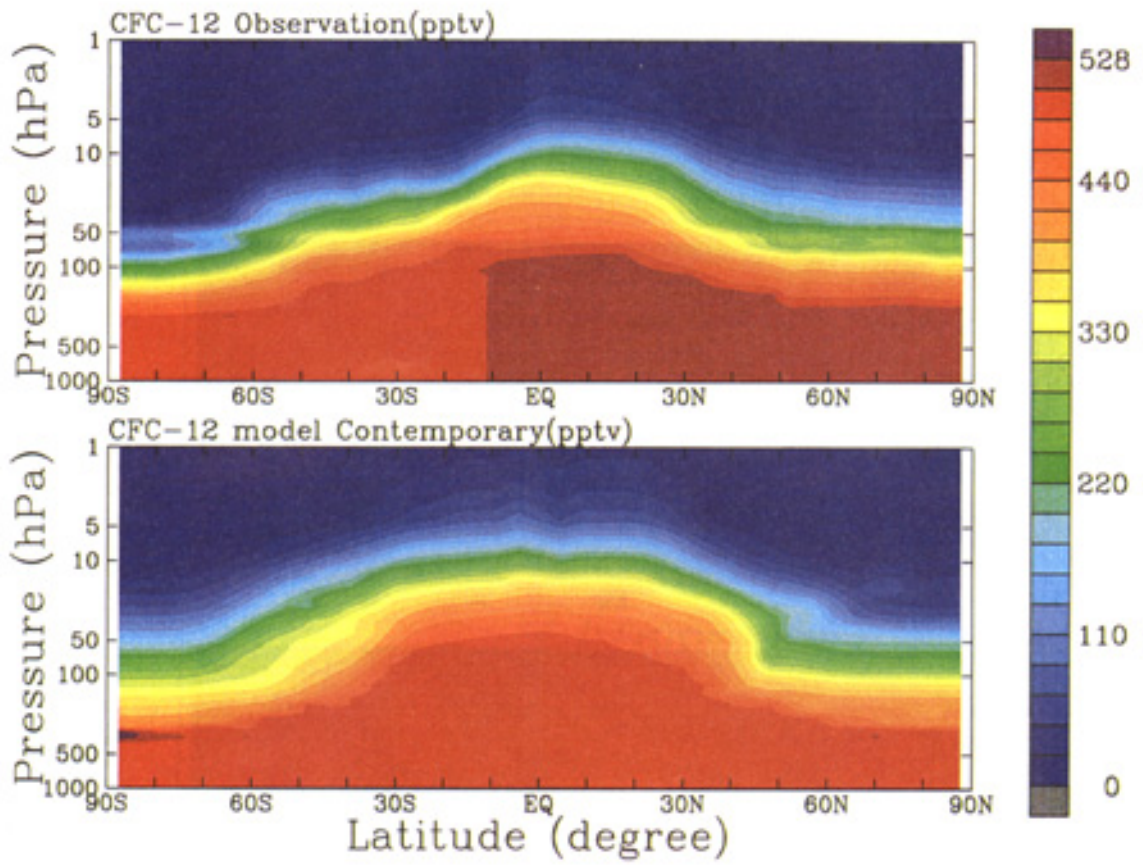

Plate 4. CTM-estimated and observed distribution of CFC-12 (pptv) used in the radiative calculations for the September-October contemporary period.

To validate CTM-based radiative forcings with observation-based forcings, we have estimated the forcings for CH_4, N_2O, and CFC-12 based on the observed measurements [*Minschwaner et al.*, 1998]. Plates 2, 3, and 4 show that CTM distributions of CH_4, N_2O, and CFC-12 for the September-October present-day atmosphere compare well with the observation data. In Plates 2-4 the observed distributions of gases in the stratosphere were derived from vertical profiles measured by the Cryogenic Limb Array Etalon Spectrometer (CLAES) onboard UARS [*Minschwaner et al.*, 1998]. Measurement times were extended from March 1992 to January 1993. Observed concentrations for CH_4 [*Tans et al.*, 1992] and for N_2O, and CFC-12 [*Montzka et al.*, 1992] in the troposphere, assumed to be height independent, were obtained from 1991 to1992 measurements from a surface network operated by the Climate Monitoring and Diagnostics Laboratory (CMDL). Plates 2-4 show the latitudinal variations for N_2O (less than 1% pole to pole) but is significant for CH_4 (about 9% pole to pole) and CFC-12 (about 6%). In general, the values from the model agree well with the observations. Plates 2 and 3 also show the CTM concentrations of CH_4 and N_2O for preindustrial time, which were used in the model-based and observation-based radiative forcing calculations for the preindustrial time.

2.4. Spectroscopic Data

Line parameters for H_2O, CO_2, O_3, CH_4, N_2O, and SF_6 were based on the HITRAN-1992 database [*Rothman et al.*, 1992]. The HITRAN database does not provide the hot bands for SF_6. In this study the total radiative forcings for SF_6 were assumed to be 3.4 times the value estimated on the basis of HITRAN-1992 data set [*Myhre and Stordal*, 1997; *Grossman et al.*,1993]. A newer version of HITRAN database, HITRAN-1996, has also been released. *Pinnock and Shine* [1998] have shown that the effects of updated HITRAN database on calculations of radiative forcing for CO_2, CH_4, N_2O, and O_3 is less than 1%. Absorption cross-section data for CFC-11,-12,-13,-113,-114,-115, HCFC-22, and CF_4 were taken from *McDaniel et al.* [1991]. The absorption data for CCl_4 and CH_3CCl_3 were taken from *Fisher et al.* [1990]. H-1301 absorption data were from *Person and Polo* [1961], and data for HFC-245fa were made available by H. Magid of Allied Signal Inc. The infrared spectral data for the remainder of the gases were provided by M. Hurley of the Ford Motor Company; detailed information about these spectral data can be found in the work of *Pinnock et al.* [1995] and *Christidis et al.* [1997], and comparisons have also been made therein with other published works.

2.5. Description of Radiative Transfer Models

The radiative forcing calculations are performed with a broadband model (BBM) and a narrow band model (NBM). The BBM is based on the longwave band model of *Briegleb* [1992a]. This is a uniform 100 cm^{-1} band model that calculates infrared fluxes due to H_2O, CO_2, O_3, CH_4, N_2O, and CFC-11 and -12. The gas transmissions are computed by a modified Malkmus function. Gas overlapping in the same 100 cm^{-1} interval is approximated by random overlap. Cloud particle scattering is

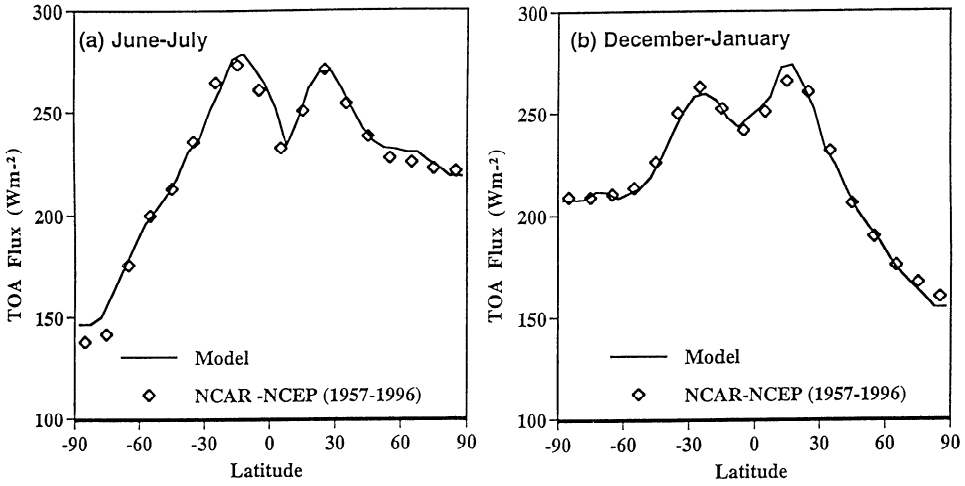

Figure 1. Comparison of the narrowband model (NBM) top of atmosphere infrared fluxes with the National Center for Environmental Prediction/National Center for Atmospheric Research (NCEP/NCAR) reanalysis estimates for (a) June-July and (b) December-January. Modeled values were calculated using the narrow band radiative transfer model initialized with temperature, greenhouse gas distributions, and clouds as discussed in the text. The NCEP/NCAR estimates are averaged for the period 1957-1996.

ignored. The BBM was modified for our purposes in this paper to include the HCFCs and HFCs. An angular integration over the upward and downward hemispheres is performed for all the gases using Guassian quadrature over 12 angles. As shown in section 3, the radiative forcing for optically thin limit gases such as the halocarbons would be underestimated if calculated using a constant diffusivity factor approximation for the angular integration.

The narrowband model (NBM) is a Malkmus random band model of band width 10 cm^{-1} for H_2O and 5cm^{-1} for CO_2, O_3, CH_4, and N_2O. These intervals were chosen because spectrally integrated infrared fluxes compare favorably with reference line-by-line calculations. The 5cm^{-1} transmissions are averaged for each 10 cm^{-1} interval, and gases are overlapped using the random overlap approximation. The bandwidth for other gases considered here was assumed to be 10 cm^{-1}.

One measure of accuracy in the radiative forcing calculations is how well the background infrared fluxes are simulated. While upward and downward fluxes throughout the atmosphere are not available, we can compare computed and estimated/observed fluxes at the top of the atmosphere (TOA). Particularly important is whether the effect of high clouds in the deep tropics is simulated. Figure 1 shows the NBM-estimated TOA outgoing infrared fluxes for December-January and June-July periods compared to the 40 year National Center for Environmental Prediction/National Center for Atmospheric Research (NCEP/NCAR) reanalysis estimates [*Kalnay et al.*, 1996]. While the latter are based on model calculations for the reanalysis input, the values are within 5-10 Wm^{-2} compared to ERBE measurements over the 1985-1988 period [*Minschwaner et al.*, 1998]. At all latitudes for the two periods shown, the NBM-computed fluxes agree to within 10 Wm^{-2} of the NCEP/NCAR estimates. Both periods show how the relative minimum in the deep tropical outgoing fluxes is well simulated in the NBM calculations.

In the BBM and NBM the shortwave radiative fluxes are obtained from the delta-Eddington model [Briegleb, 1992b]. Eighteen spectral intervals are used from 0.2 to 5.0 μm, with seven shortwaves of 0.35 μm to represent ozone absorption: one in the visible (0.35 to 0.70 μm), and 10 in the near infrared (0.70 to 5.00 μm) for O_2, H_2O, and CO_2 absorption. Molecular and cloud droplet scattering are included. The model gives an accurate approximation to shortwave scattering and absorption based on comparisons with higher resolution and more accurate scattering calculations.

The thickness of vertical layers was assumed to be 100 mbar in the troposphere, decreasing to 10-20 mbar near the tropopause and lower stratosphere. The layer thickness in the middle and upper stratosphere was assumed to be about 3 km. Higher vertical resolution than this yields a negligible change in the radiative forcing values.

3. Radiative Forcing Calculations Based on Single Global and Annual Mean Atmosphere

There are number of published studies that report radiative forcing calculations. However, many problems arise when comparing these studies, mainly because these calculations were carried out for the wide range of assumptions and data sets. For example, in some studies, stratospheric adjustment was not included. In other studies, radiative forcing was calculated for clear-sky conditions. Radiative forcing should be calculated with the stratospheric adjustment and using appropriate temperature, water vapor, ozone, and cloud conditions [*Albritton et al.*, 1995; *Granier et al.*, 1999]. Intercomparison problems also arise due to details of radiative schemes. A wide variety of radiative transfer models are currently in use, ranging from line-by-line models to broadband approaches. Intercomparison of results from these models show that the uncertainties in the radiative forcing for doubling of CO_2 could be as large as 10% [*Luther and Fouquart*, 1984]. In this section we estimate the sensitivity of greenhouse gas radiative forcing to a number of the assumptions discussed above, including the use of the BBM versus the NBM, clear-sky versus cloudy sky forcing, instantaneous versus adjusted forcing, diffusivity factor-based versus angular integration-based forcings, and constant versus realistic profile-based forcings.

For this section of the analysis we used a single GAM vertical profile for temperature, H_2O, O_3, CH_4, N_2O, and

Table 1. Global and Annual Mean (GAM) Atmospheric Profile Used for Radiative Forcing Calculations for the Single Atmosphere Profile.

Pressure, mbar	Temperature, K	H_2O,* g/g	O_3,* g/g	CH_4, ppbv		N_2O, ppbv		CFC-11, ppbv	CFC-12, ppbv
				1765	1992	1765	1992	1992	1992
0.10	231.46	3.99E-06	1.79E-06	100.50	150.10	0.42	0.49	0.00	0.01
0.50	259.67	3.95E-06	3.27E-06	121.50	195.60	1.85	2.14	0.00	0.21
1.00	263.02	3.91E-06	5.12E-06	146.60	253.90	4.66	5.32	0.00	1.16
2.00	255.05	3.72E-06	8.90E-06	197.30	374.10	12.35	13.70	0.00	6.78
4.00	241.41	3.39E-06	1.23E-05	284.20	586.90	33.38	36.49	0.01	34.86
6.00	234.62	3.16E-06	1.34E-05	348.70	755.50	58.26	63.52	0.11	74.71
8.00	230.81	3.02E-06	1.38E-05	393.70	877.00	81.17	88.86	0.67	113.47
10.00	228.20	2.93E-06	1.41E-05	425.40	963.90	100.03	110.28	2.24	148.25
15.00	224.28	2.78E-06	1.21E-05	475.30	1103.60	135.44	152.55	13.59	206.54
20.00	221.22	2.71E-06	1.08E-05	509.00	1196.40	159.72	177.99	36.53	261.56
25.00	218.85	2.65E-06	9.18E-06	532.70	1264.50	177.21	197.81	60.68	291.88
30.00	216.92	2.59E-06	7.49E-06	550.90	1314.50	190.02	212.51	85.30	315.28
40.00	214.12	2.44E-06	5.01E-06	577.60	1384.50	207.93	233.06	125.44	342.67
50.01	212.05	2.29E-06	3.33E-06	596.30	1439.70	220.86	247.93	166.93	361.91
60.01	210.43	2.13E-06	2.83E-06	611.80	1507.00	231.01	259.48	174.72	375.64
80.01	208.40	2.14E-06	2.04E-06	632.40	1544.00	245.38	276.13	206.27	396.28
100.01	207.30	2.19E-06	1.43E-06	646.30	1584.10	252.93	284.82	213.45	414.07
120.01	209.47	2.36E-06	1.01E-06	651.60	1600.80	259.12	289.61	245.66	427.44
140.01	211.30	2.84E-06	7.86E-07	660.30	1622.90	261.43	294.93	231.76	426.74
160.02	213.71	3.70E-06	5.78E-07	665.00	1637.30	264.99	298.35	240.36	435.99
180.02	216.62	5.14E-06	4.62E-07	669.50	1648.30	266.85	301.02	248.22	450.87
200.02	219.22	1.03E-05	3.45E-07	672.90	1657.80	269.12	303.28	253.99	447.41
220.02	222.06	1.89E-05	2.74E-07	675.20	1665.00	270.42	304.76	256.93	451.91
240.02	224.66	3.23E-05	1.83E-07	677.30	1668.30	271.35	305.80	265.05	454.99
260.03	227.49	5.60E-05	8.27E-08	678.70	1674.00	271.93	306.48	262.38	457.19
280.03	230.54	8.52E-05	5.15E-08	684.40	1678.90	273.55	307.43	267.91	463.86
300.03	233.37	1.24E-04	5.15E-08	682.20	1682.20	273.18	307.92	268.06	463.54
400.04	247.33	4.57E-04	5.15E-08	684.90	1688.50	273.84	308.67	269.17	464.39
500.05	258.31	1.04E-03	5.15E-08	687.70	1693.80	274.25	309.14	269.48	464.71
600.06	266.68	1.88E-03	5.15E-08	690.50	1698.80	274.54	309.47	269.70	464.92
700.07	273.75	3.52E-03	5.15E-08	693.10	1703.50	274.74	309.71	269.87	465.09
800.08	279.31	6.27E-03	5.15E-08	695.80	1708.00	274.90	309.87	270.00	465.23
900.09	284.49	8.17E-03	5.15E-08	698.10	1713.60	275.02	310.02	270.11	465.33
1000.10	289.38	1.06E-02	5.15E-08	701.40	1752.60	275.07	310.05	270.32	465.45

The preindustrial and 1992 distributions for all gases except for CO_2 were derived on the basis of chemical transport model results. CO_2 concentrations were assumed constant throughout the atmosphere at preindustrial and present-day 1992 levels of 278 and 356 ppmv. The concentrations of CFC-11 and CFC-12 during preindustrial times were assumed to be zero. Read 3.99E-06 as 3.99×10^{-6}.

* Mass mixing ratio.

cloudiness (Table 1), which were based on latitudinal and seasonal averaging of the data discussed above.

3.1. Broadband Model Versus Narrowband Model Results for Radiative Forcing

Although line-by-line model (LBLM) calculations are generally considered to provide the most accurate results for radiative forcings, they are too computationally expensive to calculate the cloudy sky radiative forcings. This is particularly true for the adjusted radiative forcing, which requires several radiative transfer calculation for each single atmospheric profile. On the other hand, NBM calculations are computationally less expensive than LBLM calculations and more accurate than the BBM results and have been shown to produce greenhouse gas forcings within a few percent of that LBLM calculations [*Freckleton et al.*, 1996]. In previous studies, we employed a BBM to calculate the radiative forcings for a number of greenhouse gases [*Naik et al.*, 2000; *Li et al.*, 2000; *Good et al.*, 1998; *Minschwaner et al.*, 1998]. In order to evaluate the accuracy of the BBM results, we compare the cloudy sky instantaneous radiative forcing results of the BBM with the NBM (Table 2). The major difference between the NBM (spectral resolution 5-10 cm^{-1}) and the BBM (spectral resolution 100 cm^{-1}) is the treatment of the spectral overlapping. Table 2 also compares the effects of overlap with H_2O, O_3, CO_2, CH_4, and N_2O.

Table 2 shows that with the exception of CFC-114, HCFC-123, HFC-245fa, CF_4, CH_2Br_2, and CHF_2Br, BBM radiative forcings are smaller than NBM results. The radiative forcing results estimated by two models are the same for HFC-23, HFC-161, SF_6, and CH_3Br. The differences in radiative forcings for the three major greenhouse gases (CO_2, CH_4, and N_2O) are about 8%. However, differences in the halocarbon and perfluorocarbon radiative forcing between the two models are as large as 68% (e.g., CF_4). Because CF_4 has a very strong narrow spectral region centered near 1283 cm^{-1}, it overlaps with the bands of CH_4, N_2O, and H_2O. As shown in Table 2, the BBM is unable to capture these overlapping effects. The BBM 100 cm^{-1} spectral interval is large enough to mask over "windows" that some gases with narrow bands have, thus reducing their radiative forcing.

Halocarbons mostly overlap with water vapor because they absorb in the window region (between 800 and 1200 cm^{-1}). However, some of the halocarbons also have a overlapping effects with the absorption bands of CO_2, CH_4, N_2O, and O_3. Table 2 shows that the spectral overlapping of these gases with H_2O and other gases is poorly treated in a BBM, since many of the halocarbons have absorption bands much less than 100 cm^{-1} wide. For example, CCl_4 has a very localized absorption band centered at 790 cm^{-1}, which overlaps with the wing of the 665 cm^{-1} band of CO_2. In the case of H-1301, which has a very narrow band centered at 1085 cm^{-1}, the overlap occurs mainly

Table 2. Impact of Overlapping Effects on Instantaneous Cloudy Sky Radiative Forcing Calculated Using the Narrowband Model (NBM) and Broadband Model (BBM).

Gas	Radiative Forcing			No H_2O*		No O_3*		No CO_2*		No CH_4*		No N_2O*	
	NBM	BBM	BBM-NBM	NBM	BBM	NBM	BBM	NBM	BBM	NBM	BBM	NBM	BBM
	Wm^{-2}	Wm^{-2}	%	%	%	%	%	%	%	%	%	%	%
CO_2	0.084	0.078	-8	12	13	7	8	0	0	6	5	6	6
CH_4	0.005	0.004	-8	52	52	0	0	0	0	0	0	16	10
N_2O	0.035	0.032	-8	25	25	0	0	14	19	6	7	0	0
Chlorofluorocarbons (CFCs)													
CFC-11	0.268	0.255	-5	10	10	1	7	2	2	0	0	0	0
CFC-12	0.322	0.300	-7	9	9	1	5	0	1	1	0	1	1
CFC-13	0.246	0.188	-24	17	17	1	6	0	3	0	6	0	7
CFC-113	0.307	0.301	-2	11	10	7	6	0	1	1	1	1	1
CFC-114	0.298	0.305	2	12	11	8	6	0	0	2	1	2	2
CFC-115	0.216	0.202	-6	14	17	2	2	0	0	2	5	2	6
Chlorocarbons (CCs)													
CCl_4	0.148	0.106	-28	16	11	0	2	6	50	0	0	0	0
CH_3CCl_3	0.079	0.077	-3	12	11	3	7	49	50	1	0	1	1
Hydrochlorofluorocarbons (HCFCs)													
HCFC-22	0.213	0.192	-10	13	14	1	4	0	3	1	1	1	2
HCFC-123	0.189	0.192	1	17	17	1	1	0	1	5	4	5	4
HCFC-124	0.211	0.201	-5	18	18	1	3	7	7	4	5	4	6
HCFC-141b	0.149	0.128	-14	12	12	1	4	7	19	1		1	1
HCFC-142b	0.184	0.171	-7	15	15	1	2	0	0	1	2	1	3
HCFC-225ca	0.260	0.239	-8	18	21	7	6	14	14	2	6	2	6
HCFC-225cb	0.271	0.264	-3	12	12	2	5	8	9	2	1	2	2
Hydrofluorocarbons (HFCs)													
HFC-23	0.255	0.256	0	21	22	2	3	4	3	4	1	4	3
HFC-32	0.168	0.149	-11	18	19	6	19	4	4	1	1	1	1
HFC-125	0.256	0.226	-12	19	23	1	1	6	5	3	7	3	7
HFC-134	0.188	0.178	-5	19	20	2	2	0	1	2	1	2	3
HFC-134a	0.207	0.217	5	20	21	2	5	2	2	5	4	5	4
HFC-143	0.130	0.115	-12	13	14	3	16	1	1	1	1	1	2
HFC-143a	0.161	0.138	-14	24	28	0	0	2	4	4	11	4	11
HFC-152a	0.121	0.117	-3	21	20	1	2	1	0	1	0	1	2
HFC-161	0.037	0.037	0	20	18	25	27	0	1	0	0	0	0
HFC-227ea	0.325	0.279	-14	24	28	0	0	2	4	4	11	4	11
HFC-236fa	0.259	0.226	-13	31	37	1	1	9	9	4	11	4	9
HFC-245fa	0.272	0.281	3	27	25	3	8	5	4	4	3	4	4
Perfluorocarbons (PFCs)													
SF_6	0.148	0.148	0	7	7	0	1	3	1	0	0	0	0
CF_4	0.088	0.149	68	40	28	0	0	0	0	36	19	36	17
Bromocarbons (BCs)													
H-1211	0.291	0.277	-5	11	11	1	7	2	2	1	0	1	1
H-1301	0.302	0.206	-32	11	13	1	29	3	4	0	6	0	6
CH_3Br	0.008	0.008	0	41	47	3	3	25	39	6	4	6	3
CH_2Br_2	0.019	0.020	6	18	20	0	1	168	137	2	1	2	3
CHF_2Br	0.182	0.181	2	15	16	2	9	19	12	2	1	2	3
Iodocarbons (ICs)													
CF_3I	0.279	0.267	-4	13	10	9	24	6	4	2	0	2	1
CF_3CF_2I	0.290	0.257	-12	17	20	0	1	5	5	1	5	1	5

Radiative forcings are for an increase of a 1 ppbv (0-1 ppbv) for halocarbons, 5 ppmv for CO_2 (350-355 ppmv), 10 ppbv for CH_4 (1714-1724 ppbv) and N_2O (311-321 ppbv).

* The values are the increase in the net flux due to overlap reduction for individual gas.

with H_2O. Table 2 shows that the BBM was incapable of taking into account these localized overlapping effects.

3.2. Clear-Sky Versus Cloudy Sky Radiative Forcing

Clouds play an important role in the calculation of greenhouse gas radiative forcings. Table 3 shows that clouds could reduce the adjusted clear-sky radiative forcings by as much as 35%, consistent with the results of *Pinnock et al.* [1995] and *Myhre and Stordal* [1997], due to a smaller upward irradiance during cloudy sky conditions. The clouds have a smaller effect on the radiative forcing of CO_2 than on other greenhouse gases, because the total optical depth is already large due to higher CO_2 concentrations and strong absorption in the 15 μm band. On the other hand, halocarbons absorb in the weak line limit and CH_4 and N_2O between weak and strong line limits; therefore optical depths for non-CO_2 gases are much smaller, and hence the impact of clouds on their radiative forcing is larger (Table 3).

Table 3. Estimated Radiative Forcings Using the Narrowband model (NBM) in Combination With a Global and Annual Mean (GAM) Background Atmosphere.

Gas	Lifetime (year)	Radiative Forcing (Wm^{-2})	Clear Sky (%)	Instantaneous (%)	Constant Diffusivity (%)	Model-Derived Vertical Profile (%)
CO_2	variable	0.073	14.1	14.8	0.3	
CH_4	12.2	$4.75x10^{-3}$	28.5	2.5	1.2	-1.4
N_2O	120	$3.37x10^{-2}$	24.7	3.6	0.4	-1.9
			Chlorofluorocarbons (CFCs)			
CFC-11	45	0.280	31.2	-4.2	-1.9	-10.2
CFC-12	100	0.340	33.5	-5.3	-2.5	-4.9
CFC-13	640	0.260	33.9	-5.4	-4.5	
CFC-113	85	0.319	32.3	-3.6	-3.0	-8.1
CFC-114	300	0.310	33.0	-3.6	-3.4	-5.0
CFC-115	1700	0.227	33.8	-4.7	-5.4	-1.4
			Chlorocarbons (CCs)			
CCl_4	35	0.153	28.2	-3.1	-4.2	-16.7
CH_3CCl_3	4.8	0.079	26.6	-0.2	-5.4	-15.1
			Hydrochlorofluorocarbons (HCFCs)			
HCFC-22	11.8	0.223	33.1	-4.4	-3.9	-2.3
HCFC-123	1.4	0.199	32.7	-5.0	-3.9	-26.9
HCFC-124	6.1	0.223	32.9	-5.1	-4.0	-10.5
HCFC-141b	9.2	0.155	32.0	-3.6	-3.9	-13.4
HCFC-142b	18.5	0.194	34.1	-5.4	-3.7	-13.4
HCFC-225ca	2.1	0.268	31.7	-3.1	-4.6	-21.8
HCFC-225cb	6.2	0.284	32.4	-4.5	-4.5	-11.7
			Hydrofluorocarbons (HFCs)			
HFC-23	243	0.268	33.6	-4.7	-4.5	-3.0
HFC-32	5.6	0.173	33.9	-2.9	-3.8	-7.6
HFC-125	32.6	0.271	33.1	-5.4	-4.9	-5.5
HFC-134	10.6	0.195	33.3	-3.5	-4.9	-6.7
HFC-134a	13.6	0.217	32.8	-4.7	-4.5	-5.6
HFC-143	3.8	0.135	35.0	-3.5	-3.5	-12.5
HFC-143a	53.5	0.171	32.9	-5.6	-5.4	-3.7
HFC-152a	1.5	0.127	34.5	-4.3	-3.8	-20.4
HFC-161	0.25	0.036	34.8	2.4	-1.9	-39.0
HFC-227ea	36.5	0.346	32.3	-6.0	-5.7	-3.2
HFC-236fa	226	0.274	31.8	-5.3	-5.5	-0.6
HFC-245fa	7.69*	0.284	32.1	-4.1	-5.3	-5.8
			Perfluorocarbons (PFCs)			
SF_6	3200	0.156	33.4	-5.3	-2.5	
CF_4	50000	0.091	26.6	-3.1	-4.6	
			Bromocarbons (BCs)			
H-1211	11	0.306	32.7	-4.7	-2.9	-15.9
H-1301	65	0.318	34.3	-5.0	-3.8	-9.2
CH_3Br	0.7	0.007	26.0	2.0	-3.5	
CH_2Br_2	0.41	0.019	28.5	0.2	-5.0	
CHF_2Br	7.0	0.182	32.4	-2.1	-6.6	
			Iodocarbons (ICs)			
CF_3I	0.005	0.285	33.4	-2.2	-5.4	
CF_3CF_2I	0.005	0.306	32.3	-5.2	-4.2	

The reference values listed in column 3 are the cloudy sky adjusted radiative forcing with the angular integration due to a constant concentration change throughout the atmosphere. Columns 4-7 are the calculated percentage changes under the different condition as compared to reference case. Radiative forcings are for an increase of a 1 ppbv (0-1 ppbv) for halocarbons, 5 ppmv for CO_2 (350-355 ppmv), 10 ppbv for CH_4 (1714-1724 ppbv), and N_2O (311-321 ppbv).

* *Naik et al.* [2000].

3.3. Instantaneous Versus Adjusted Radiative Forcing

The sign and the magnitude of the effect of stratospheric adjustment on radiative forcing due to the stratospheric adjustment depends on whether the net effect of both the stratospheric and the tropospheric forcings leads to a heating or a cooling of the stratosphere, with a resultant increase or decrease in thermal infrared emissions from the lower stratosphere to the troposphere, respectively [*Schimel et al.*, 1996]. Halocarbons absorb predominantly in the window region (750-1250 cm^{-1}), in the linear line limit; therefore in the stratosphere they absorb the upwelling radiation from the troposphere and increase the heating rate of the stratosphere. When the stratospheric temperature is allowed to reach equilibrium, the stratosphere warms. Stratospheric warming

increases the downward radiative flux into the troposphere, resulting in an increase in the radiative forcing. Table 3 shows that the NBM-estimated instantaneous cloudy sky radiative forcings for halocarbons are up to 6% lower than the adjusted radiative forcing. Increasing the amounts of strongly absorbing gases results in enhanced CO_2, CH_4, and N_2O stratospheric cooling. For this reason, the instantaneous radiative forcings for CO_2, CH_4, and N_2O are 15%, 3%, and 4% higher, respectively, than the adjusted radiative forcings.

3.4 Diffusivity Factor-Based Versus Angular Integration-Based Radiative Forcings

In the original version of the radiative transfer model used in this study [*Briegleb*, 1992a], the angular integration for the radiative calculations was approximated by a band-independent diffusivity factor. For CO_2, CH_4, N_2O, H_2O, and O_3, a diffusivity factor of 1.66 was assumed, while for chlorofluorocarbons, diffusivity was assumed to be a function of total optical depth [*Ramanathan et al.*, 1985]. Instead of using a diffusivity factor approximation we estimated the angular integration within each spectral interval with a 12-point Gaussian quadrature. The explicit angle integration allowed the use of angle-dependent surface emissivities. A NBM-estimated diffusivity-based and explicit angular-integration-based radiative forcings are compared in Table 3. The inaccuracy in radiative forcing for well-mixed and strongly absorbing greenhouse gases, such as CO_2, CH_4, and N_2O, due a diffusivity factor approximation is small (1% or less). However, a diffusivity factor approximation employed by *Briegleb* [1992a] for the weakly absorbing halocarbons underestimates the radiative forcings by as much as 7%.

3.5. Constant Vertical Profile-Based Versus Realistic Vertical Profile-Based Radiative Forcings

The greenhouse gases in radiative forcing calculations are often assumed to be evenly distributed throughout the atmosphere and over the globe. Observed vertical profiles of greenhouse gases, however, reveal a decrease in concentrations with height, depending on the lifetime of the gas. Gases with lifetimes of a few years or more are generally well mixed in the troposphere, but in the stratosphere, the vertical transport is much slower. In addition, for many of the greenhouse gases the photochemical loss rate increases with height above the tropopause. The combined effects of transport and photochemistry cause most greenhouse gas concentrations to decrease with height in the stratosphere. Here we compare the radiative forcing calculated with evenly distributed concentrations with the forcing calculated using 2-D CTM-estimated vertical changes in greenhouse gas concentrations [see *Naik et al.*, 2000, Figure 1]. Radiative forcing calculations were done for the adjusted and cloudy sky conditions using the NBM discussed in section 2.5. As shown in Table 3, both the uniform mixing ratio profiles and the 2-D CTM model-estimated profiles with decreasing concentration in height yield about the same radiative forcings for CH_4 and N_2O; the difference is less than 1%. The reason for this is that the scale heights of the mixing ratios for CH_4 and N_2O are sufficiently large to yield nearly the same changes in stratospheric concentrations for these gases. However, the global and annual mean radiative forcings estimated using realistic vertical profiles are considerably lower for all CFCs, HCFCs, and HFCs studied here. Table 3 clearly shows that the reduction in the radiative forcing is not the same for all gases. Table 3 also indicates that the total lifetime of a gas itself is not a good indicator to estimate the reduction in radiative forcings, which occurs when using actual vertical profiles. For example, the total lifetimes of HFC-141b and HFC-142b are 10 and 18 years, respectively [*Naik et al.*, 2000]. However, the reductions in radiative forcing due to these gases occurs when using the decreasing vertical profiles are the same for both gases (13%). Moreover, it is the combination of stratospheric and tropospheric lifetimes that determines the vertical profile of a gas and hence the reductions in radiative forcing. If a gas has a tropospheric lifetime of 2-3 years, it will generally be well mixed in the troposphere. For these gases, it is the stratospheric lifetime that is more important in determining the vertical profiles. As shown in Table 3, the percent reductions are quite significant for the gases with a lifetime of 2 years or less, e.g., HFC-161 (39%, 0.3 years), HFC-152a (20%, 2 years), and HCFC-123 (27 %, 1.4 years) (in parentheses the first value is a percent reduction in radiative forcing (Table 3), and the second value is a total lifetime of a gas [*Naik et al.*, 2000]). On the other hand, percent reduction in radiative forcing is quite small for long-lived CFCs, HFCs, and HCFCs, for example, CFC-115 (1.5%, 1700 years), HCFC-22 (2%, 12 years), and HFC-236fa (0.5 %, 209 years). These radiative forcing results show the importance of varying vertical profiles of greenhouse gas concentrations when calculating radiative forcings. In section 4 we show that the radiative forcing is sensitive not only to the vertical profile but also to latitudinal and the seasonal variations in greenhouse gas concentrations and atmospheric characteristics.

4. Radiative Forcing With Realistic Latitudinal and Seasonal Profiles of Greenhouse Gases and Atmospheres

Radiative forcings presented in section 3 were calculated on the basis of a single GAM atmospheric profile. However, radiative forcing changes with region and season as well, mainly due to spatial and time variations in temperature, H_2O, O_3, and cloudiness, as well as greenhouse gas distribution. *Myhre and Stordal* [1997] and *Freckleton et al.* [1998] found that the calculated global mean radiative forcing, based on spatially varying atmospheric profiles, is quite different for some gases than the radiative forcing calculated on the basis of the single GAM atmospheric profile. Specifically, *Myhre and Stordal* [1997] found that the global and annual mean radiative forcing for several well-mixed greenhouse gases calculated from a single atmospheric profile could be 5-10% in error compared to the calculations using monthly and regional resolution 2.5° x 2.5° atmospheric profiles. However, they found that the error in radiative forcing due to temporal and longitudinal variations in well-mixed greenhouse gases was small (less than 1%). They also concluded that it was the latitudinal variation that must be represented to reduce the majority of the error in radiative forcing. Extending this conclusion, *Freckleton et al.* [1998] show that the error in the radiative forcing for some well-mixed greenhouse gases calculated from the single atmospheric profile could be reduced by an order of magnitude or more by using three atmospheric profiles, one representing the tropics and one representing each of the northern and southern extratropics.

The purpose of this section is to provide global and annual mean radiative forcing calculated from changes in H_2O, O_3, greenhouse gas concentrations, temperature, and cloud distribution as a function of latitude and season. Of particular importance for our calculations in this section are the latitudinal and seasonal variations in the vertical profiles of greenhouse gases. The latitudinal and seasonal data used for the calculations have already been discussed in sections 2.2 and 2.3 and shown in Plates 1-4 for the September-October time period. The calculations were carried out on a 5° latitude grid from 87.5° S to 87.5° N, for four standard seasons. The latitudinal mean data for the background atmosphere for each season is the

Table 4. NBM-Based Cloudy Sky Adjusted Radiative Forcing in Wm^{-2} Due to a Constant Change in Surface Concentrations Calculated With a Narrowband Model Using the CTM-Based Latitudinal and Seasonal (LAS) Greenhouse Gas Profiles.

Gas	LAS	GAM-LAS	WMO [*Granier et al.*, 1999]	
	Wm^{-2}	%	Wm^{-2}	WMO-LAS %
CO_2	0.075*	-2.7	0.076	0.9
CH_4	$4.67x10^{-3}$	-0.3	$3.70x10^{-3}$+	-21.3
N_2O	$3.29x10^{-2}$	-0.4	$3.70x10^{-2}$+	11.3
		Chlorofluorocarbons (CFCs)		
CFC-11	0.240	4.9	0.25	4.3
CFC-12	0.302	7.0	0.32	6.0
CFC-13	0.245*	6.0	0.25	2.0
CFC-113	0.284	2.1	0.30	5.7
CFC-114	0.290	1.5	0.31	7.1
CFC-115	0.214	4.4	0.21 (0.26)‡	-2.0 (21)
		Chlorocarbons (CCs)		
CCl_4	0.125	1.3	0.10	-20.2
CH_3CCl_3	0.065	2.7	0.06	-8.1
		Hydrochlorofluorocarbons (HCFCs)		
HCFC-22	0.205	6.4	0.22	7.5
HCFC-123	0.143	1.4	0.20	39.5
HCFC-124	0.195	2.1	0.22	12.8
HCFC-141b	0.131	2.6	0.14	7.1
HCFC-142b	0.164	2.6	0.20	22.1
HCFC-225ca	0.207	1.3	0.27	30.3
HCFC-225cb	0.245	2.3	0.32	30.6
		Hydrofluorocarbons (HFCs)		
HFC-23	0.248	4.5	0.20	-19.4
HFC-32	0.155	2.9	0.13	-16.3
HFC-125	0.249	3.0	0.23	-7.5
HFC-134	0.176	3.3	0.18	2.3
HFC-134a	0.200	2.6	0.19	-4.9
HFC-143	0.115	2.6	0.13	13.1
HFC-143a	0.160	3.0	0.16	0.3
HFC-152a	0.097	3.8	0.13	33.6
HFC-161	0.022	2.7	0.03	38.9
HFC-227ea	0.322	4.3	0.30	-6.6
HFC-236fa	0.264	3.4	0.28	6.2
HFC-245fa	0.261	2.6	0.23	-12.0
		Perfluorocarbons (PFCs)		
SF_6	0.494*	7.5	0.52	5.3
CF_4	0.089*	2.6	0.08	-10.1
		Bromocarbons (BCs)		
H-1211	0.251	2.6	0.30	19.7
H-1301	0.273	5.5	0.32	17.1
CH_3Br	0.007*	2.9	0.01	37.9
CH_2Br_2	0.019*	3.7	0.01	-46.5
CHF_2Br	0.174*	4.8	0.14	-19.4
		Iodocarbons (ICs)		
CF_3I	0.268*	6.3	0.23	-14.2
CF_3CF_2I	0.293*	4.2	0.26	-11.5

LAS values are also compared with the GAM (global and annual mean) atmosphere-based values as well as with those of recent WMO assessment values [*Granier et al.*, 1999]. Radiative forcings are for an increase of a 1 ppbv (0-1 ppbv) for halocarbons, 5 ppbv for CO_2 (350-355 ppmv), 10 ppbv for CH_4 (1714-1724 ppbv) and N_2O (311-321 ppbv).

* Calculated by assuming uniform distribution with height and latitude.

+ Based on *Schimel et al.* [1996]

‡ Note that there was a typographical error in WMO [*Granier et al.*, 1999] reported value for CFC-115; the actual value was 0.21 Wm^{-2}, whereas reported values was 0.26 Wm^{-2}.

average of the 2 months of data covering the solstice or equinox. To calculate the global mean radiative forcings, latitudinal averaging is done by area weighting. For this set of calculations, 2-D CTM-estimate greenhouse gas distributions were employed. The CTM was not used to calculated the distributions for CO_2, CFC-13, perfluorocarbons (PFCs), iodocarbons (ICs) and three bromocarbons (CH_3Br, CH_2Br_2, and CHF_2Br). Therefore these gases were assumed to be distributed uniformly in altitude and latitude for each season. The adjusted radiative forcing calculations were done for cloudy sky conditions using the NBM. Table 4 compares the global and annual mean radiative forcing calculated using latitudinal and seasonal (LAS) mean greenhouse gas profiles and atmospheric conditions with the realistic single GAM atmosphere case.

Radiative forcing for most of the greenhouse gases is noticeably sensitive to the LAS mean greenhouse gas distributions and atmospheric conditions. Estimated forcings for CO_2, CH_4, and N_2O based on a single GAM profile were lower than the LAS case, whereas the single-profile forcings were higher for halocarbons and perfluorocarbons, consistent with the findings of *Freckleton et al.* [1998]. This is due to the fact that the tropopause height in the GAM profile is relatively higher than the LAS case, and hence the stratospheric adjustment takes place at a lower pressure level. Thus the stratospheric adjustment will be large compared to LAS case, producing a larger cooling for CO_2, CH_4, N_2O, and smaller warming for other gases. This results in a difference of up to 7% between LAS- and GAM-based forcings. The differences were significantly higher (5-7%) for CFC-11, CFC-12, HFC-22, HFC-23, and H-1301, mainly because these gases decay much more rapidly in the stratosphere. Similar results have also been found by *Freckleton et al.* [1998], who estimated the differences in radiative forcings between GAM and LAS cases to be about 6-7% for CFC-11 and CFC-12. For other gases with higher stratospheric lifetimes, the differences are relatively small. Most of these gases have very small stratospheric sinks, which yield nearly the same changes in stratospheric concentrations for both the LAM and the GAM cases. The difference in radiative forcings due to a constant change in SF_6 is slightly higher than CFC-11 and CFC-12. This occurs as a result of both the higher concentrations in the stratosphere, and the differences in tropopause height between GAM and LAS cases, as discussed above.

The changes in radiative forcing from preindustrial to present-day times for CO_2, CH_4, N_2O, and for total CFCs as a function of time and latitude are shown in Plate 5. As evident in this figure, changes in greenhouse gas radiative forcings vary with latitude and season. The radiative forcing due to CO_2 was more homogeneous than other gases, as CO_2 overlaps more strongly with water and is less influenced by clouds. The largest CO_2 forcing occurs in the subtropical summer, where lower water vapor amount and comparatively clear-sky are found. Additionally, during summer the difference between surface temperature and tropopause is large, leading to further enhancement of the greenhouse effect. *Kiehl and Briegleb* [1993] and *Myhre and Stordal* [1997] found similar effects in their three-dimensional simulations.

5. UARS-Based Versus Model-Based Radiative Forcings

In a recent study, *Minschwaner et al.* [1998] used Upper Atmosphere Research Satellite (UARS) data in combination with a BBM to calculate the radiative forcing for CH_4, CFC-12, and N_2O. In this study we revise the UARS-based radiative forcing estimates for CH_4, N_2O, and CFC-12 using a more accurate approach, namely combining an NBM with stratospheric UARS observations and surface-based tropospheric observations. The observational data used for this set of calculations have already been discussed in detail in section 2.4. The radiative forcing is calculated for an increase in trace gas concentrations from preindustrial time (1750) to

Table 5. NBM-Estimated Adjusted Cloudy-Sky Radiative Forcing in Wm^{-2} Due to Changes in Greenhouse Gas Concentrations From Preindustrial time (1750) to the Present Day (1992).

GAS	Concentration* (ppbv)		This Study			WMO [*Granier et al.*,1999]	
	Preind. (1765)	Current (1992)	Model-Based Gas Concentration Wm^{-2} (1)	Observed-Based Gas Concentration Wm^{-2} (2)	Difference % (2) – (1)	Wm^{-2} (3)	Difference % (3) – (1)
CO_2	278,000	356,000	1.308+	1.3083	0	1.322	+1
CH_4	700	1,714	0.578	0.604	+3	0.500	-13
N_2O	275	311	0.117	0.121	+3	0.119	+2
CFC-11	0	0.268	0.064			0.067	+3
CFC-12	0	0.503	0.152	0.148	-2	0.161	+7
CFC-113	0	0.082	0.023			0.025	+9
CFC-114	0	0.020	0.006			0.006	0
CFC-115	0	0.010	0.001			0.001	0
CCl_4	0	0.132	0.017			0.013	-23
CH_3CCl_3	0	0.135	0.009			0.008	-11
FCFC-22	0	0.100	0.020			0.022	+10
H-1211	0	0.007	0.002			0.002	0
H-1301	0	0.003	0.001			0.001	0
SF_6	0	0.032	0.016+			0.017	6
CF_4	0	0.070	0.006+			0.006	0
Total			2.320			2.27	+2.2

The forcings are calculated using model-based gas distributions. *WMO* [1999] reported values and the percent difference between WMO and model-based radiative forcings are also given in columns 7 and 8.

* *Schimel et al.* [1996].

+ Calculated by assuming uniform distribution with height and latitude.

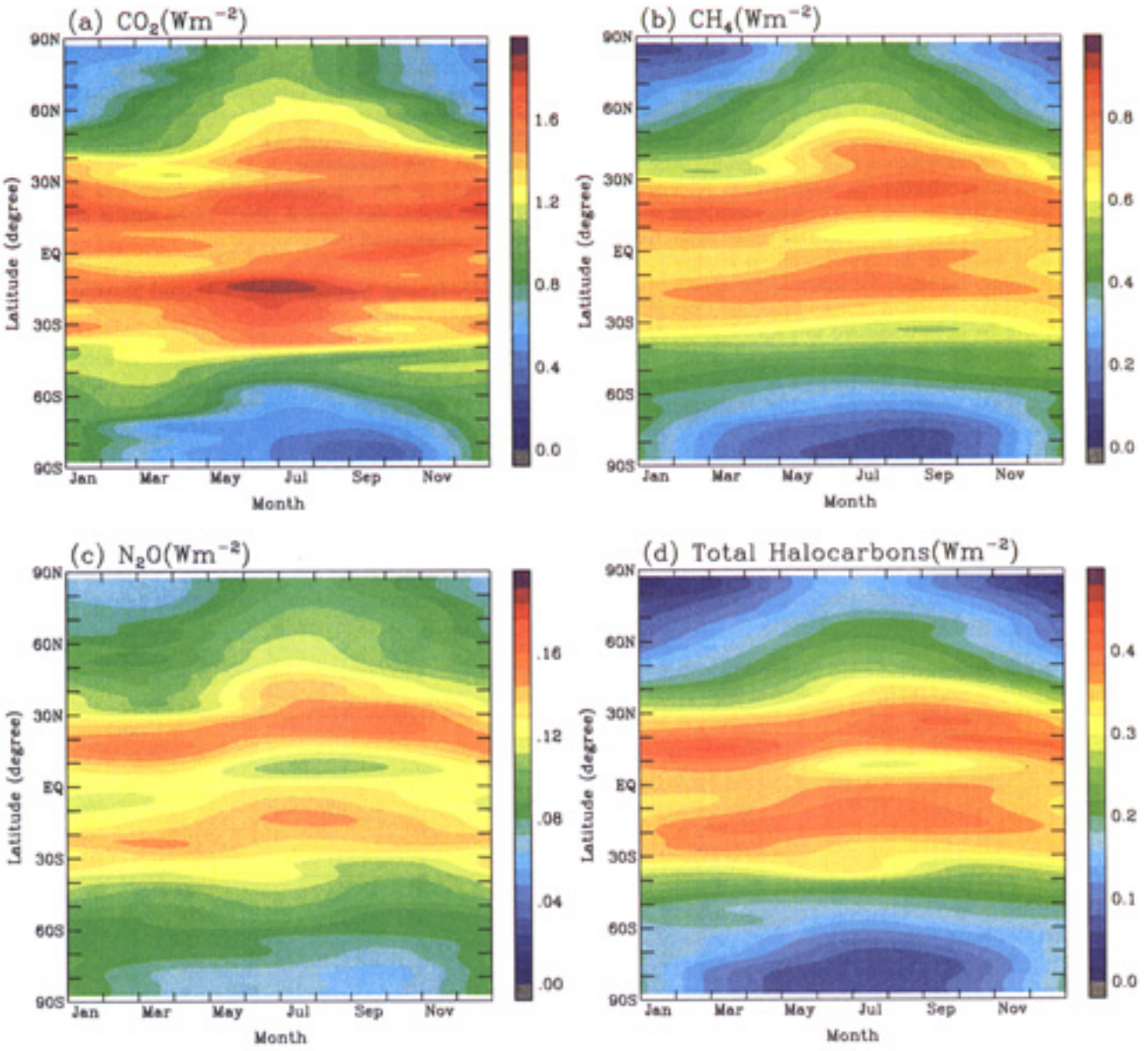

Plate 5. Estimated seasonal and latitudinal dependent changes in the radiative forcing (Wm^{-2}) for the period 1765-1992 for (a) CO_2, (b) CH_4, (c) N_2O, and (d) CFCs.

contemporary time (1992). Since there is no observed data available for the preindustrial time, 2-D CTM distributions of CH_4 and N_2O were combined with the observation-based data for these radiative transfer calculations.

Observation-based radiative forcing are 0.60, 0.12, and 0.15 Wm^{-2} for CH_4, N_2O, and CFC-12, respectively (Table 5). Radiative forcing based on the observed distributions of CH_4 and N_2O is 3% higher, and CFC-12 is about 3% lower, compared to the forcing based on CTM distributions. Our NBM radiative forcings results for CH_4, N_2O and CFC-12 are 9%, 8%, and 12% higher than the *Minschwaner et al.* [1998] BBM results, which is likely related to the differences in preindustrial concentrations, width of spectral intervals, and in treatment of angular radiances. *Freckleton et al.* [1998] also estimated the radiative forcings for CFC-12 using the UARS observation data, and our estimated forcing results were the same as estimated by *Freckleton et al.* [1998].

6. Comparison With Other Research Studies

In this section we compare our NBM adjusted cloudy sky forcings based on the realistic greenhouse gas and atmosphere profiles with other most recent estimates of forcings [*Granier et al.*, 1999; *Schimel et al.*, 1996; *Myhre et al.*, 1998]. Table 4 compares the radiative forcing for a doubling of CO_2 and for a change in surface concentrations of 10 ppbv for CH_4 and N_2O, and 1 ppbv for other greenhouse gases, whereas Table 5 compares the radiative forcings for major greenhouse gases from preindustrial time to date (year 1992).

Although our estimated radiative forcing of 3.7 Wm^{-2} for a doubling of CO_2 compares well with the recent estimates by *Myhre et al.* [1998] and *Pinnock et al.* [1995], it is about 16 % lower than the value given by *Schimel et al.* [1996]. Possible reasons for the differences in forcing are the stratospheric adjustment and shortwave radiative forcings. Both of these forcings are negative and hence lower the net radiative forcing for CO_2. As we have shown earlier, GAM atmosphere-based adjusted radiative forcings for CO_2 were about 15% lower than the instantaneous forcings. Shortwave absorption by CO_2 occurs mostly in the stratosphere, which reduces the shortwave radiation reaching the tropopause. The estimated shortwave forcing is only about 5% of the difference in net flux for CO_2 doubling, consistent with the GCMs results [*Cess et al.*, 1993]. The estimated radiative forcing for CO_2 since preindustrial time was 1.31 Wm^{-2}, about 16% lower than *Schimel et al.* [1996] but only 1% lower than the most recent estimates by *Myhre et al.* [1997]. We estimate that the uncertainty in our model-derived radiative forcing for CO_2 is less than 10%, which is much smaller than for the other gases.

The NBM radiative forcing due to the 2-D CTM-based CH_4 concentration change from preindustrial time to the present was 0.58 Wm^{-2}, although this value is consistent with other most recent NBM-based estimates [*Freckleton et al.*, 1998; *Myhre et al.*, 1998], but 20-23% higher than the *Schimel et al.* [1996]. As discussed by *Ramanathan et al.* [1987], band model-estimated forcing due to CH_4 is generally higher, because they poorly characterize absorption and emissions by CH_4 along inhomogeneous paths. The NBM is most accurate for weak-line and strong-line limits; however, the present abundance of CH_4 yields absorption between these two limits. *Ramanathan et al.* [1987] compared the several model results for CH_4 (including the Malkmus radiation model used in this study) with LBLM calculations and found that all band models overestimate the CH_4 radiative forcing, with the Malkmus model producing the smallest error of about 11% for the radiative flux at the tropopause. On the basis of *Ramanatan et al.* [1987], we conclude that our NBM-estimated CH_4 forcing might be in error by 11%.

For N_2O the 2D CTM-based estimated radiative forcing using the NBM over the period 1765-1992 was 0.12 Wm^{-2} (Table 4). Again, the NBM value is consistent with recent estimates by *Myhre et al.* [1998] but 20 % lower than the *Schimel et al.* [1996] estimates. We estimate that the uncertainty in N_2O forcing could be as large as 10% based on the spatial and temporal variations and different radiation schemes.

Except for CFCs and a few other halocarbons, the estimated radiative forcings for other halocarbons differ by more than 10% from the values given in recent WMO assessment report [*Granier et al.*, 1999], ranging as high as 58% for HCFC-161. The reasons for the large differences from WMO-reported values are unclear. WMO radiative forcings for most of these halocarbons are unchanged from recent IPCC assessment value

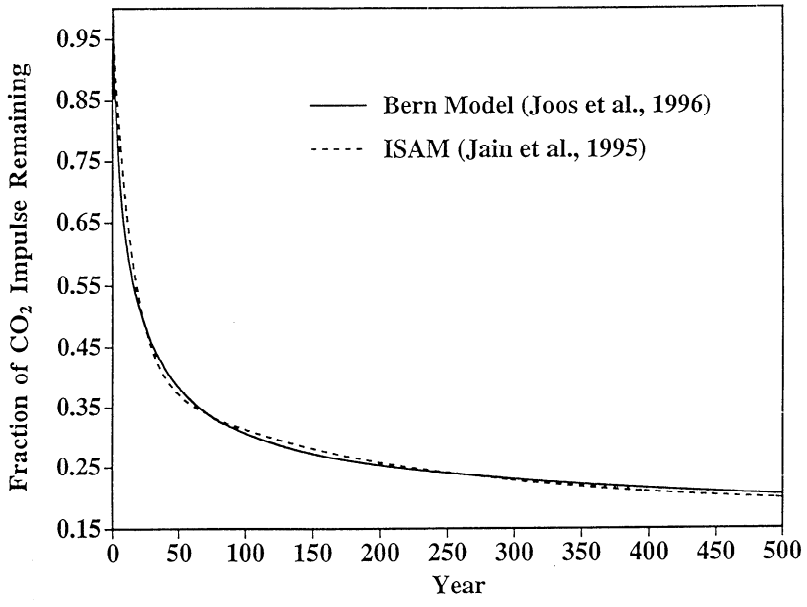

Figure 2. Comparison of Integrated Science Assessment Model (ISAM) [*Jain et al.*, 1995] estimated response to a pulse input of CO_2 with that of Bern model [*Joos et al.*, 1996].

Table 6. Estimated Global Warming Potentials (GWPs) Based on the Lifetime Given in Table 3 and Radiative Forcings Given in Table 4 for 20, 100, and 500 years time horizons.

Gas	Time Horizon in Years				
	20	100			500
	This Study	This Study	WMO [*Granier et al.*, 1999]	% Difference	This Study
CH_4	72	28	24	14	9
N_2O	296	340	360	6	188
		Chlorofluorocarbons (CFCs)			
CFC-11	6100	4700	4600	-2	1700
CFC-12	9800	10600	10600	0	5200
CFC-13	10000	14600	14000	-4	17000
CFC-113	5800	6000	6000	0	2700
CFC-114	7100	9700	9800	1	8700
CFC-115	6000	9100	10300	13	12700
		Chlorocarbons (CCs)			
CCl_4	2700	1800	1400	-22	600
CH_3CCl_3	500	160	140	-12	50
		Hydrochlorofluorocarbons (HCFCs)			
HCFC-22	4900	1900	1900	0	590
HCFC-123	280	90	120	33	28
HCFC-124	1800	590	620	5	180
HCFC-141b	2000	690	700	1	220
HCFC-142b	4300	2000	2300	15	640
HCFC-225ca	460	140	180	28	45
HCFC-225cb	1600	500	620	24	160
		Hydrofluorocarbons HFCs			
HFC-23	15000	19600	14800	-24	15900
HFC-32	3500	1100	880	-20	350
HFC-125	6700	4300	3800	-12	1400
HFC-134	3400	1200	1200	0	390
HFC-134a	4400	1800	1600	-11	560
HFC-143	1100	350	370	6	110
HFC-143a	6900	5800	5400	-7	2100
HFC-152a	480	150	190	26	46
HFC-161	25	8	-	-	2
HFC-227ea	6300	4400	3800	-14	1500
HFC-236fa	7200	9500	9400	-1	7400
HFC-245fa	3000	1000			320
		Perfluorocarbons (PFCs)			
SF_6	14600	22500	22200	-1	33200
CF_4	4400	6800	5700	-16	10600
		Bromocarbons (BCs)			
H-1211	2900	1100	1300	18	340
H-1301	6800	6300	6900	10	2500
CH_3Br	11	4	5	25	1
CH_2Br_2	10	3	1	-67	1
CH_2F_2Br	1200	390	470	20	120
		Iodocarbons (ICs)			
CF_3I	1	<1	<1	0	<1
CF_3CF_2I	1	<1		-	<1

The percent difference in GWPs for 100 year time horizon evaluated in this study and those reported by WMO [*Granier et al.*, 1999] is also given.

[*Schimel et al.*, 1996] estimates, except that for forcings have been increased by a factor of 1.14 to account for a change in the revised forcing for CFC-11. Note that the IPCC-reported estimates for most of the replacement compounds have not been amended since their first assessment [*Shine et al.*, 1990], and the forcings were reported relative to CFC-11. WMO-reported values for the CFCs, SF_6 and CF_4 were based on revised estimates by *Myhre et al.* [1998], and our values for these compounds are in good agreement with those of *Myhre et al.* [1998]. WMO-reported radiative forcings for few HFCs (HFC-134, HFC-161, and HFC-236fa), bromocarbons (except for H-1301), and iodocarbons were reproduced from *Christidis et al.* [1997] after a simple scaling to account for the decrease in the stratosphere concentrations. In contrast, our estimates are based on a consistent set of radiative transfer calculations.

The estimated total radiative forcings due to changes in the major greenhouse gases from preindustrial time to the present day is 2.32 Wm^{-2}, only about 2-3% higher than the most recent estimates [*Granier et al.*, 1999; *Myhre et al.*, 1998; *Hansen et al.*, 1997]; however, the differences for the individual gases are as large as 23% (Table 5). The uncertainties in halocarbon radiative forcings could be much higher than the other major

greenhouse gases. The potential sources of uncertainties are the spectroscopic data and the spatial and vertical distributions of these gases.

7. Global Warming Potentials

Global warming potential (GWP) is an important concept used to compare the relative potential effects on climate from various greenhouse gases. The GWP of a greenhouse gas as defined in IPCC [*Shine et al.*, 1990; *Albritton et al.*, 1995; *Schimel et al.*, 1996] is the time-integrated change in the radiative forcing of a gas, also known as absolute global warming potential (AGWP) of a gas, over a specified time horizon relative to that of CO_2. Calculating the GWP for a particular gas requires the radiative forcing and the temporal decay both for the gas of interest and for CO_2, the reference gas. In this study we evaluated the GWPs for the greenhouse gases studied here using our NBM-derived radiative forcings shown in Table 4. The temporal decay of a gas of interest was calculated on the basis of lifetimes shown in Table 3, which were taken from recent WMO assessment report [*Granier et al.*, 1999]. The decay for CO_2 was estimated on the basis of the carbon cycle component of our Integrated Science Assessment Model (ISAM) described by *Jain et al.* [1995]. As shown in Figure 2, the estimated decay of CO_2 based on the ISAM [*Jain et al.*, 1995] and Bern model [*Joos et al.*, 1996] are nearly the same. Both of these models were used to estimate the atmospheric CO_2 concentrations in recent IPCC assessment [*Schimel et al.*, 1996]. Because of the different CO_2 response function and CO_2 radiative forcings from recent WMO assessment [*Granier et al.*, 1999], the CO_2 AGWPs differ from the values used in recent WMO assessment [*Granier et al.*, 1999] by -3, -7, and -8% for the 20-, 100-, and 500-year time horizons, respectively. These lower CO_2 AGWPs lead to larger GWPs with for other gases as compared to *Granier et al.* [1999].

The derived GWPs for time horizons of 20, 100, and 500 years are listed in Table 6. In this table we also compare our estimated 100-year GWPs with those reported in recent WMO assessment report [*Granier et al.*, 1999]. Our GWPs for some of the gases differ notably from *Granier et al.* [1999], mainly because of the significant differences in the radiative forcings (Table 4) and CO_2 response function (Figure 2) as discussed above.

8. Conclusions

We have evaluated the radiative forcings and GWPs for a number of greenhouse gases using a consistent set of radiative transfer models, as well as spectroscopic and climate data sets. In addition, we have also evaluated the sensitivity of greenhouse gas radiative forcings to a number of simplified assumptions widely used in the past to calculate these forcings. Since many of the previous studies were not able to account for every detail required for radiative calculations, a sensitivity study would help to interpret the results of other studies.

The main conclusions of the paper can be summarized as follows:

1. The top-of-atmosphere fluxes calculated with the narrowband model (NBM) are in good agreement with the observed data. We also compared our NBM and BBM model results and found that the representation of spectral overlapping in the BBM model was unable to reproduce the NBM results for most of the greenhouse gases studied here. The differences in the instantaneous radiative forcings for two models were as large as 68% (for CF_4) for gases that have strong narrow features in their spectra.

2. We also investigated the sensitivity of the radiative forcings to clouds, stratospheric adjustment, and angular radiances. Our model results show that omitting these factors in the radiation schemes could result in forcing errors of several percent. The errors due to omitting these factors are much higher for halocarbons.

3. Our model results show that the vertical profiles of the gases are important in determining the radiative forcings; the use of height-independent vertical distributions of greenhouse gases resulted in errors of up to 39% in estimated radiative forcings for gases studied here; the errors for the short-lived compounds were particularly high. We also find that the errors in evaluated radiative forcings caused by neglecting both the seasonal and the latitudinal distributions of greenhouse gases and atmospheric conditions were much smaller than the errors due to ignoring height-independent vertical distributions.

4. Our results indicate a strong variation of greenhouse gas forcings with season and latitude, with forcing maxima in the summer subtropics. The radiative forcing of CO_2 was more homogeneous than that of other gases, as CO_2 overlaps more strongly with water vapor and is also less influenced by clouds.

5. For most halocarbons, our estimated radiative forcings are significantly different than the most recent estimated values given by WMO [*Granier et al.*, 1999]. These differences might be due to the use of a different model, the inclusion of cloudy conditions, the background atmosphere specified, and type of forcings considered, whether instantaneous or adjusted.

6. Our estimated change in radiative forcing due to increases in major greenhouse gas concentrations for the period 1765-1992 is 2.32 Wm^{-2}. This value is only about 2-3% higher than the recent WMO estimates [*Granier et al.*, 1999]; however, the differences for individual gases were as large as 23%.

7. Radiative forcing based on the UARS-measured distributions of CH_4 and N_2O are 3% higher, and forcings for CFC-12 is 3% lower as compared to the forcing based on CTM distributions.

8. Finally, the calculated GWPs for most of the greenhouse gases differ significantly from most recent estimated values by WMO [*Granier et al.*, 1999], mainly because of differences in our evaluated radiative forcings.

Acknowledgments. This research was supported in part by grants from U.S. National Science Foundation (grant NSF DMF 9711624), U.S. Environmental Protection Agency (CX825749-01), and from related support on tools and methods of assessment from BER Program, U.S. Department of Energy (DEFG02-99ER62741). The National Center for Atmospheric Research is sponsored by the National Science Foundation. We thank K. Hayhoe for helpful comments.

References

Albritton, D.L., R.G. Derwent, I.S.A. Isaksen, M. Lal, and D.J. Wuebbles, Trace gas radiative forcing indices, in *Climate Change 1994: Radiative Forcing of Climate Change and An Evaluation of the IPCC IS92 Emission Scenarios*, edited by J.T. Houghton et al., 163-203, Cambridge Univ. Press, New York, 1995.

Anderson, G. P., S. A. Clough, F. X. Kneizys, J. H. Chetwynd, and E. P. Shettle, AFGL atmospheric constituent profiles (0-120 km), *AFGL Tech. Rep., AFGL-TR-86-0110*, 43 pp., Air Force Phillips Lab., Hansom Air Force Base, Mass., 1986.

Briegleb, B., Longwave model for thermal radiation in climate studies, *J. Geophys. Res.*, *97*, 11,475-11,485, 1992a.

Briegleb, B., Delta-Eddington approximation for solar radiation in the NCAR Community Climate Model, *J. Geophys. Res.*, *97*, 7603-7612, 1992b.

Cess R. D. et al., Uncertainties in carbon dioxide radiative forcing in atmospheric general circulation models, *Science*, *262*, 1252-1255, 1993.

Christidis, N., M.D. Hurley, S. Pinnock, K.P. Shine, and T.J. Wallington, Radiative forcing of climate change by CFC-11 and possible CFC replacements, *J. Geophys. Res*, *102*, 19,597-19,609, 1997.

Dessler A. E., K. Minschwaner, E. M. Weinstock, E. J. Hintsa, J. G. Anderson, and J. M. Russell III, The effects of tropical cirrus clouds on the abundance of lower stratospheric ozone, *J. Atmos. Chem.*, *23*, 209-220, 1996.

Fisher, D.A., C.H. Hales, W.-C. Wang, M.K.W. Ko, and N.D. Sze, Model calculations of the relative effects of CFCs and their replacements on global warming, *Nature*, *244*, 513-516, 1990.

Freckleton, R. S., S. Pinnock, and K. P. Shine, Radiative forcing of halocarbons: A comparison of line-by-line and narrow-band models using CF_4 as an example, *J. Quant. Spectrosc. Radiat. Transfer*, *55*, 763-769, 1996.

Freckleton, R.S., E.J. Highwood, K.P. Shine, O. Wild, K.S. Law, and M.G. Sanderson, Greenhouse gas radiative forcing: Effects of averaging and inhomogeneities in trace gas distribution, *Q. J. R. Meteorol. Soc.*, *124*, 2099-2127, 1998.

Good, D.A., J.S. Francisco, A.K. Jain, and D.J. Wuebbles, Lifetimes and global warming potentials for dimethyl ethers and for fluorinated ethers: CH_3OCF_3 (E143a), CHF_2OCHF_2 (E134), CHF_2OCF_3 (E125), *J. Geophys. Res*, *103*, 28,181-28,186, 1998.

Granier C., K.P. Shine, J.S. Daniel, J.E. Hansen, S. Lal, and F. Stordal, Climate effects of ozone and halocarbon changes, in *Scientific Assessment of Ozone Depletion: 1998*, *WMO Rep. 44*, World Meteorol. Organ. Global Ozone Res. and Monit. Proj., Geneva, 1999.

Grossman, A. S., K. E. Grant, and D. J. Wuebbles, Radiative forcing calculations for SF6 and CH4 using a correlated k-distribution transmission model, *LLNL Tech. Rep., UCRL-ID-115042*, 12 pp., Lawrence Livermore Natl. Lab., Livermore, Calif., 1993.

Hansen, J. E., M. Sato, and R. Ruedy, Radiative forcing and climate responses, *J. Geophys. Res.*, *102*, 6831-6864, 1997.

Jain, A. K., H. S. Kheshgi, M. I. Hoffert, and D. J. Wuebbles, Distribution of radiocarbon as a test of global carbon cycle models, *Global Biogeochem. Cycles*, *9*, 153-166, 1995.

Joos, F., M. Bruno, R. Fink, U. Siegenthaler, T. F. Stocker, C. le Quéré, and J. L. Sarmiento, An efficient and accurate representation of complex oceanic and biospheric models of anthropogenic carbon uptake, *Tellus, Ser. B*, *48*, 397-416, 1996.

Kalnay, E., et al., The NCEP/NCAR 40-year reanalysis project, *Bull. Am. Meteorol. Soc.*, *77*, 437-471, 1996.

Kiehl, J. T., and B. Briegleb, The relative role of sulfate aerosols and greenhouse gases in climate forcing, *Science*, *260*, 311-314, 1993.

Kotamarthi, V. R., D. J. Wuebbles, and R. A. Reck., Effects of nonmethane hydrocarbons on lower stratospheric and upper tropospheric chemical climatology in a two-dimensional zonal average model, *J. Geophy. Res.*, *104*, 21,537-21,547, 1999.

Levy, H., II, J. D. Mahlman, W. J. Moxim, and S. C. Liu, Tropospheric ozone: The role of transport, *J. Geophys. Res.*, *90*, 3753-3772, 1985.

Li, Z., Z. Tao, V. Naik, D. A. Good, J. Hansen, G. Jeong, J. S. Francisco, A. K. Jain, and D. J. Wuebbles, Global warming potential assessment for $CF_3OCF{=}CF_2$, *J. Geophys. Res.*, *105*, 4019-4029, 2000.

Luther, F. M., and Y. Fouquart, The intercomparison of radiation codes in climate models (ICRCCM), *Rep. WCP-93*, 37 pp., World Meteorol. Organ., Geneva, 1984.

McDaniel, A. H., C. A. Cantrell, J. A. Davidson, R. E. Shetter, and J. G. Calvert, The temperature dependent infrared absorption cross-sections for chlorofluorocarbons: CFC-11, CFC-12, CFC-13, CFC-14, CFC-22, CFC-113, CFC-114, CFC-115, *J. Atmos.Chem.*, *12*, 211-227, 1991.

McPherson, R., K. H. Bergman, R. K. Kistler, G. E. Rasch, and D. S. Gordon, The NMC operational global data assimilation system, *Mon. Weather Rev.*, *107*, 1445-1461, 1979.

Minschwaner, K., R. W. Carver, B. P. Briegleb, and A. E. Roche, Infrared radiative forcing and atmospheric lifetimes of trace species based on observations from UARS, *J. Geophys. Res.*, *103*, 23,243-23,253, 1998.

Montzka, S. A, et al., Nitrous oxide and halocarbons division, in *Climate Monitoring and Diagnostics Laboratory No. 20, Summary Report 1991*, edited by E. E. Ferguson and R. M. Rosson, NOAA Environ. Res. Lab., Boulder, Colo., 1992.

Myhre, G., and F. Stordal, Role of spatial and temporal variations in the computation of radiative forcing and GWP, *J. Geophys. Res.*, *102*, 11,181-11,200, 1997.

Myhre, G., E. J. Highwood, K. P. Shine, and F. Stordal, New estimates of radiative forcing due to well mixed greenhouse gases, *J. Geophys. Res. Lett.*, *25*, 2715-2718, 1998.

Naik, V., A. K. Jain, K. O. Patten, and D. J. Wuebbles, Consistent sets of atmospheric lifetimes and radiative forcings on climate for CFC replacements: HCFCs and HFCs, *J. Geophys. Res.*, *105*, 6903-6914, 2000.

Oltmans, S. J., Surface ozone measurements in clean air, *J. Geophys. Res.*, *86*, 1174-1180, 1981.

Person, W. B., and S. R. Polo, Infrared intensities of the fundamental frequencies of CF_3Br, *Spectrochim. Acta*, *17*, 101-111, 1961.

Pinnock, S., and K. P. Shine, The effects of changes in HITRAN and uncertainties in the spectroscopy on infrared irradiance calculation, *J. Atmos. Sci.*, *55*, 1950-1964, 1998.

Pinnock, S., M.D. Hurley, K.P. Shine, T.J. Wallington, and T.J. Smyth, Radiative forcing of climate by hydrochlorofluorocarbons and hydrofluorocarbons, *J. Geophys. Res*, *100*, 23,227-23,238, 1995.

Ramanathan, V., R. J. Cicerone, H.B. Singh, and J. T. Kiehl, Trace gas trends and their potential role in climate change, *J. Geophys. Res., 90*, 5547-5566, 1985.

Ramanathan, V., et al., Climate-chemical interactions and effects of changing atmospheric trace gases, *Rev. Geophys.*, *25*, 1441-1482, 1987.

Rossow, W. B., and R. A. Schiffer, ISCCP cloud data products, *Bull. Am. Meterol. Soc.*, *72*, 2-20, 1991.

Rothman, L. S., et al., The HITRAN molecular database: Editions of 1991 and 1992, *J. Quant. Spectrosc. Radiat. Transfer*, *48*, 469-507, 1992.

Schimel, D., et al., Radiative forcing of climate change, in *Climate Change 1995: The Science of Climate Change*, edited by J.T. Houghton et al., 65-131, Cambridge Univ. Press, New York, 1996.

Shine, K.P., R.G. Derwent, D.J. Wuebbles, and J-J. Morcrette, Radiative forcing of climate, in *Climate Change, The IPCC Scientific Assessment*, edited by J.T. Houghton, G. J. Jenkins, and J. J. Ephraums, 41-68, Cambridge Univ. Press, New York, 1990.

Stephens, G. L., and C. M. R. Platt, Aircraft observations of the radiative and microphysical properties of stratocumulus and cumulus cloud fields, *J. Clim. Appl. Meteorol.*, *26*, 1243-1269, 1987.

Tans, P. P., T. J. Conway, E. J. Dlugokencky, K. W. Thoning, P. M. Lang, K. A. Masarie, P. Novelli, and L. Waterman, Carbon cycle division, in *Climate Monitoring and Diagnostics Laboratory No. 20, Summary Report 1991*, edited by E. E. Ferguson and R. M. Rosson, NOAA Environ. Res. Lab., Boulder, Colo., 1992.

Waters, W.C., J. P. Pinto, and Y.L. Yung, Microwave limb sounding, in *Atmospheric Remote Sensing by Microwave Radiometry*, edited by M. A. Janssen, pp. 383-496, John Wiley, New York, 1993.

World Meteorological Organization (WMO), *Scientific Assessment of Ozone Depletion: 1991*, *WMO Rep. 25*, Global Ozone Res. and Monit. Proj., Geneva, 1992.

WMO, *Scientific Assessment of Ozone Depletion: 1994*, *WMO Rep. 37*, Global Ozone Res. and Monit. Proj., Geneva, 1995.

Wuebbles, D.J., A. K. Jain, R. Kotamarthi, V. Naik, and K. O. Patten, Replacements for CFCs and Halons and their effects on stratospheric ozone, in *Recent Advances in Stratospheric Processes*, edited by T. Nathan and E. Cordero, 113-143, Res. Signpost, Kerala, India, 2000.

B.P. Briegleb, National Center for Atmospheric Research, Boulder, CO 80307.

A.K. Jain, and D.J. Wuebbles, University of Illinois, Department of Atmospheric Sciences, 105 S. Gregory Avenue, Urbana, IL 61801. (jain@atmos.uiuc.edu)

K. Minschwaner, Department of Physics, New Mexico Institute of Mining and Technology, Socorro, NM 87801.

(Received January 11, 2000; revised April 6, 2000;
accepted April 10, 2000.)